https://doi.org/10.20575/00000050
Polar Data Journal, Vol. 7, 72–88, October 2023

Ecosystem aboveground structures of an open-canopy black spruce forest in interior Alaska for ecosystem modeling

Hideki KOBAYASHI[1]*, Yongwon KIM[2], Taro NAKAI[3], Hiroki IKAWA[4], Shin NAGAI[1,8], Kyotaro NOGUCHI[5], Wei YANG[6], Akira HAMA[7], Shinji MATSUMURA[9], Kyoko IKEDA[1] and Rikie SUZUKI (Deceased)

[1] Institute of Arctic Climate and Environment Research, Research Institute for Global Change, Japan Agency for Marine-Earth Science and Technology, 3173-25 Showa machi, Kanazawa-Ku, Yokohama, Kanagawa 236-0001.

[2] International Arctic Research Center, University of Alaska, Syun-Ichi Akasofu Building 2160, Koyukuk Drive, Fairbanks, AK 99775-7340, USA.

[3] School of Forestry and Resource Conservation, National Taiwan University, No. 1, Sec. 4, Roosevelt Road, Taipei, 10319, Taiwan.

[4] Hokkaido Agricultural Research Center, National Agricultural and Food Research Organization, 1 Hitsujigaoka, Toyohira, Sapporo, Hokkaido 062-0045.

[5] Department of Forest Soils, Forestry and Forest Products Research Institute, 1 Matsunosato, Tsukuba, Ibaraki 305-8687.

[6] Center for Environmental Remote Sensing, Chiba University,1-33 Yayoi-cho, Inage-ku, Chiba, Chiba 263-8522.

[7] Graduate School of Horticulture, Faculty of Horticulture, Chiba University, 648 Matsudo, Matsudo, Chiba 271-8510.

[8] Earth Surface System Research Center, Research Institute for Global Change, Japan Agency for Marine-Earth Science and Technology, 3173-25 Showa machi, Kanazawa-Ku, Yokohama, Kanagawa 236-0001.

[9] National Research Institute for Earth Science and Disaster Resilience, 3-1 Tennodai, Tsukuba, Ibaraki 305-0006.

*Corresponding author. Hideki Kobayashi (hkoba@jamstec.go.jp)

(Received June 12, 2023; Accepted August 24, 2023)

Abstract: Recent warming trends in the Arctic and boreal regions far exceed the global average, and this trend is likely to continue in the future. To establish accurate benchmarks for models and represent the current status of carbon stocks and flows, it is essential to provide detailed descriptions of forest ecosystem structures, including understory plant communities alongside carbon flux data. In this data paper, we present a synthesis data set of aboveground forest structural characteristics.

Field campaigns were performed from 2010 to 2018 at the Poker Flat Research Range of the Geophysical Institute of the University of Alaska, Fairbanks, located on the outskirts of Fairbanks, AK, USA. The forest is a sparse evergreen needle-leaf forest. The field campaigns include tree census surveys in the years 2010 and 2014, direct measurement of tree aboveground biomass and their vertical profiles in 2012, tree leaf area index (LAI) measurement using a non-destructive method in 2018, and biomass and LAI survey of forest floor vegetation through direct sampling in 2018. The ecosystem structure data sets described in this paper are helpful for the calibration of the forest stand representations in the ecosystem and land surface models and for the validation of the simulated forest growth and stand structures. The data are available for download from the Japanese National Institute of Polar Research Arctic Data archive System, listed under Kobayashi *et al.* 2023.

1. Background and Summary

Recent warming trends in the Arctic and boreal regions greatly exceed the global average, and are likely to continue in the future[1,2]. Previous studies have provided evidence of warming based on various climate indicators and associated changes in the terrestrial ecosystem[3], including the state of permafrost (permafrost thaw)[4] and the patterns and magnitude of wildfires[5]. To date, no land surface and ecosystem models have yet achieved sufficient consideration of the complex behaviors of permafrost soil and forest systems[6]. This is due to the lack of comprehensive data sets to describe the realistic forest stand in the subarctic boreal forest, where tree stands are very sporadic, and the majority of the forest understory is directly illuminated by the sunlight. To establish accurate benchmarks for models and represent the current status of carbon stocks and flows, it is essential to provide detailed descriptions of forest ecosystem structures, including understory plant communities alongside carbon flux data. In this data paper, we present a synthesis data set of aboveground forest structural characteristics. Field campaigns were performed from 2010 to 2018 at the Poker Flat Research Range of the Geophysical Institute of the University of Alaska, Fairbanks, located on the outskirts of Fairbanks, AK, USA. The forest is a sparse evergreen needle-leaf forest (see section 2). The field campaigns include tree census surveys in the years 2010 and 2014, direct measurement of tree aboveground biomass and their vertical profiles in 2012, tree leaf area index (LAI) measurement using a non-destructive method in 2018, and biomass and LAI survey of forest floor vegetation through direct sampling in 2018.

In the forest census surveys, all tree locations, tree species, diameter at breast height (DBH), and tree heights were surveyed within a 30 m × 30 m (Figure 1 & 2) area within the flux footprint of the eddy covariance observation site (Figure 3). This survey was conducted twice, in 2010 and 2014. In the 2010 survey, we also measured the lengths of branch/shoot extensions in four directions, east, west, north, and south, to evaluate the maximum projected crown area of twenty selected trees. For direct measurement of tree aboveground biomass and their vertical profiles, sixteen black spruce

trees were chosen for sampling. During this field campaign, individual tree DBH, height, aboveground dry biomass, partitions of tree biomass (foliage/branch/stem), and total leaf area of each tree were measured (Figure 4). In addition, the vertical profiles of dead and live branch biomass, leaf area, and stem biomass were quantified. For tree LAI measurement through the non-destructive method, the landscape-scale LAI of the black spruce forest was obtained from gap fraction measurements along four parallel 200 m east–west transects (Figure 3, Table 2). The gap fraction was assessed using the Plant Canopy Analyzer (LAI-2200C, LiCOR), and LAI was calculated through inversion of the gap fraction (Table 3). The forest understory LAI and biomass were obtained through direct sampling in sixteen 0.5 m × 0.5 m quadrats. Leaf mass per area (LMA) of the seven dominant species, understory LAI, foliage and woody biomass, and species composition of the understory layer based on aboveground biomass were evaluated.

The ecosystem structure data sets described in this paper are helpful for the calibration of the forest stand representations in the ecosystem and land surface models and for the validation of the simulated forest growth and stand structures.

2. Location

The study site, named the Poker Flat Research Range (PFRR) flux observation supersite, is located in PFRR and operated by the Geophysical Institute of the University of Alaska Fairbanks (UAF) and located at 65°07′24″N, 147°29′15″W at an elevation of 210 m above sea level. The PFRR flux observation supersite was initiated as a research collaboration between the Japan Agency for Marine-Earth Science and Technology and the International Arctic Research Center (IARC) of UAF and currently serves as an observation platform of the Japanese Arctic Research Program (Arctic Challenge for Sustainability, ArCS/ArCSII). The site is also known as US-Prr in the AmeriFlux and FLUXNET communities[7,8].

The study site is a sparse evergreen needleleaf forest[7,9]. CO_2 and water fluxes and meteorological conditions have been measured from a 17 m scaffold tower since 2010. Eddy covariance systems were installed at a height of 11 m on the tower and 1.9 m on a tripod located 15 m from the tower[10]. Long-term continuous phenological and sky monitoring with time-lapse cameras (Phenological Eyes Network, PEN) has been conducted since 2011[11], and spectral reflectance measurements have been collected since 2015. A list of existing micrometeorological and plant phenology monitoring in the study site is summarized in Table 1.

The site experiences a subarctic climate with cold winters and dry, hot summers. The average daily temperatures in February and July were −20.2°C and 14.6°C, respectively, in 2011–2016. This site is situated in a discontinuous permafrost region. The active layer depth was 43 cm (maximum thaw depth of the year), and soil deeper than 43 cm was permafrost[7].

Black spruce (*Picea mariana*) is the dominant overstory tree species, and the percentage of tree cover across the landscape is less than 20%. The canopy height (cumulative basal area inflection height) is 2.91 m[7]. The age of trees evaluated through tree ring analysis (N = 27 with the radius of 25±7 mm) is from 44 to 99 years old[12]. According to above- and belowground biomass measurements, the black spruce forest stand in PFRR has high belowground biomass allocation, with belowground biomass accounting for 47% of the total biomass. In comparison, fine-root biomass was 36% of the entire root biomass[13].

The understory is occupied by shrubs, sedges, mosses, and lichens. Peat moss (*Sphagnum fuscum*) and feather moss (*Hylocomium splendens*) dominate in the understory. Northern reindeer lichen (*Cladina stellaris*) is distributed sporadically. Shrubs and sedges, such as Labrador tea (*Rhododendron groenlandicum*), bog bilberry (*Vaccinium uliginosum*), cloudberry (*Rubus chamaemorus*), cranberry (*Vaccinium oxycoccos*), bog birch (*Betula glandulosa or Betula nana*) and tussock formations of cotton grass (*Eriophorum vaginatum*) are commonly present[8,14]. Snowmelt and continuous snow cover begin in late April to May and in October[9,15], respectively. Leaf emergence of understory plants occurs soon after the snow melts, and senescence begins in the middle August[15,16].

3. Methods

3.1. Forest census survey “Tree Census”

Forest census measurements were collected from July 2 to 5, 2010, and September 8 to 11, 2014. We established a 30 × 30 m^2 plot within a flux footprint area. When setting the location of the plot, we selected a forest area far from the flux tower that closely resembled the forest around the tower. A location far from the tower was chosen because surveying trees around the tower would disturb the forest floor and adversely affect the collection of CO_2 and H_2O flux data. The coordinate system of the plot is defined with the origin at the southeast corner, the X axis (east–west coordinate axis) increasing from east to west, and the Y axis (north–south coordinate axis) increasing from south to north.

The center of the plot is located near 65º17´N, 147 º 29´W. Exact geographic coordinates will be provided by the authors upon request. Within a census plot, trees taller than 1.3 m were identified, and their horizontal positions (x, y), DBH at 1.3 m, and heights were measured. Tree heights were measured using a leveling rod. For trees exceeding the range of the leveling rod, a laser rangefinder (TruPulse, Laser Technology Inc.) was used. The plot was divided into 10 m × 10 m subplots. The locations of these subplots are shown in Figure 1.

Crown projection measurements were performed as part of the survey in 2010. Due to the limited time available, measuring all 357 trees that we measured DBH was not possible. We selected 20 representative trees within the study plot. To assess the correlation between crown size and tree

height, 20 trees were chosen across a representative range of tree heights. For crown projection, the distance from the trunk was measured in four directions, north, south, east, and west, for both green branches (Live) and dead branches (Dead). In addition, the height of the lowest green branches was recorded.

3.2. Aboveground biomass of black spruce trees "Tree_allometry"

3.2.1. Selection of trees for sampling

Tree sampling was conducted near the PFRR flux tower from August 25 to September 1, 2012. Sixteen black spruce trees were selected for destructive sampling. These trees were chosen to obtain a representative height range in the study area: minimum = 0.62 m, maximum = 6.08 m, and average = 2.81 m.

3.2.2. Outdoor measurements

Before cutting the trees, we measured their positions, heights, DBH, stem diameters at ground level, maximum crown lengths in four directions (north, south, east, and west), and the lowest height of live branches with green needles. Tree shapes were recorded through digital photography. Then, the trees were cut at ground level and immediately carried to a nearby workshop. The trees were laid on a tarpaulin to avoid the loss of materials attached to the trees. The tree stems were then cut at 50-cm intervals.

3.2.3. Indoor measurements

The 50-cm long stem sub-samples (hereinafter referred to as stem pieces) from each tree were investigated using the following procedures. First, all branches originating from the stem were categorized as "Dead" or "Live" based on whether green needles were present on the branches. Then, the diameters of these branches at the stem were measured using calipers and micrometer gauges. After these measurements, all branches were cut from the stem, and the live and dead branches were stored separately. The diameter of the stem piece was measured at three points (bottom, middle and top of the stem piece). Finally, the fresh weights of all elements associated with a stem piece were measured through the following procedures. The fresh stem weight was measured using a spring balance, and the total weights of the "Dead" and "Live" branches originating from a stem piece were measured with a digital scale after removing all needles. We repeated these procedures for all stem pieces collected from all sixteen sampled trees.

3.2.4. Dry weight

The dry weights of the stem, dead and live branches, and green needles were evaluated, and the dry to fresh weight fraction was determined. To measure this fraction, stem pieces at the bottom, middle, and top height levels of all sixteen tree samples were placed in a dryer at 70°C for at least

five days until the stems were completely dried. The dry to fresh weight fractions of branches were quantified using eleven branch sub-samples. Those eleven samples were selected from five trees to account for differences among individuals, “Dead” or “Live” status, and branch height (0.5–5.5 m). After fresh weight measurement, the branch samples were placed in a dryer for five days, and then their dry weights were measured. From the resulting dry to fresh weight fractions (dry weight/fresh weight), the average and the standard deviation of the dry and fresh fractions obtained from the eleven branch samples were 0.65 +/- 0.09. As the variation (coefficient of variation = 14%) of the fraction of dry weight/fresh weight was small, we decided to apply the average dry to fresh weight fraction to all branch elements regardless of “Dead” or “Live”. In contrast to stems and branches, the dry weights of all needles were directly measured after 48–72 hours in a dryer at 70°C.

3.2.5. Leaf mass per area and total leaf area of black spruce needles

Leaf mass per area (LMA) is defined as leaf dry mass per unit leaf area (g m^{-2}). LMA was quantified from needle samples that were collected separately from tree branches. We collected 839 fresh needles for LMA calculation. The total leaf area of those needles was measured and calculated from the average length (l) and diameter (d) of the needles, assuming that the needle shape can be approximated as a cylinder. The length of all 839 needle samples was directly measured using calipers and micrometer gauges. Needle diameter was challenging to measure due to the very small sizes of the needles. We selected 40 needles and measured their minimum and maximum diameters with a micrometer gauge and then averaged all of those measurements, assuming that the cross-section can be approximated as a circle. The total leaf area of 839 needles was then calculated using the formula for a cylinder: leaf area = $0.5d^2 \pi l$. Finally, LMA was calculated as the ratio of total leaf area quantified as described above and the dry mass of needles measured after drying at 70°C for 48 hours.

3.3. Forest gap fraction and overstory LAI “Overstory_LAI”

3.3.1. Gap fraction measurements

The LAI of the black spruce forest was obtained from gap fraction measurements taken along four parallel 200 m east–west transects (labeled A, B, C, and D in Figure 3). The measurements were collected on July 24, 2018, from 15:28 (Alaskan Standard Time, AKST) to 16:59 (AKST) under completely clear sky conditions. Two Plant Canopy Analyzers (LAI-2200C, Li-COR) were used to obtain above- and below-canopy radiation. The below-canopy light intensity was measured approximately 0.3 m above the ground surface, and measurement was repeated along four parallel north–south transects. Each transect was 200 m in length, and measurements were taken at an interval of 10 m, which is roughly four times the mean canopy height and approximately the footprint of the LAI-2200C sensor. A 17 m tall flux tower was located approximately 100 m northeast of the four transects. One LAI-2200C sensor was located at the top of the flux tower to

measure incoming light intensity and other LAI-2200C sensors provided incoming light intensity data below the canopy along the transects. A pair of LAI-2200C sensors were matched by placing both sensors at the top of the tower before the transect measurements. A 45° field-of-view cap was used in this study according to the recommendations of past studies[17,18]. The azimuthal orientation of each pair of LAI-2200C instruments was 157.5° clockwise from true north (true north = 0° and true south = 180°). In each transect, we collected measurements twice (from east to west and west to east) to confirm that the results were consistent. The two values obtained at each sampling point were then averaged. Finally, we conducted 21 below-canopy light-intensity samplings along each transect. Table 2 summarizes the times and corresponding solar directions at which the measurements were performed. The gap fraction at each sampling point was derived from the below-canopy light intensity divided by the above-canopy light intensity measured from the top of the tower.

The LAI calculation algorithm of the LAI-2200C requires additional sky information, including hemispherical skylight intensity (without direct sunlight), and fraction of direct solar radiation to correct light scatterings within the vegetation canopy[19]. The fraction of direct solar radiation was measured before and after transect measurements. The LAI-2200C sensor was pointed in the nadir direction above a white Halon diffuse reflectance standard panel (99% reflectivity, 25 cm × 25 cm, Spectralon, Labsphere Inc.). The LAI-2200C sensor measured the light reflected by the white panel, which represented incoming blue radiation. Then, direct sunlight was blocked from reaching the panel. The fraction of diffuse blue radiation was calculated by dividing the shaded reading by the unshaded reading from the ring 1 of the LAI-2200 device. Hemispherical skylight intensity was measured using a 270° field-of-view cap at the top of the tower before and after measurement along the four transects; the cap's orientation was adjusted to block direct solar beams.

3.3.2. LAI calculation

The landscape overstory LAI was computed through the following steps using all gap fraction data from the four transects (N = 21 × 4). First, the effective plant area index (PAI), which includes foliage clumping larger than the crown scale, was computed using the gap fraction inversion algorithm[19]. Then, LAI was computed using the following equation[20,21]:

$$LAI = \gamma(1- \alpha)PAI$$

where γ and α are shoot-level clumpings and the ratio of the woody fraction to the total plant area. γ was set to 1.58, according to the spherical average of the photographed silhouette area to the total needleleaf area ratio (STAR = 0.158) quantified previously and converted to γ ($\gamma = (4STAR)^{-1}$)[20,21]. We set α to 0.16, assuming that the wood fraction is the same as in Canadian old-growth black spruce forests[20,21].

3.4. Leaf area index and leaf mass per area (LMA) of the understory plants "Understory_LAI_biomass"

The LAI of understory plants was obtained through direct sampling. Sampling was performed on July 21 and 23, 2018, when understory LAI was at its maximum. We established sixteen 0.5 m × 0.5 m quadrats. All aboveground plant species were cut and sorted into seven dominant types, namely cloudberry, cotton grass, bog bilberry, cranberry, bog birch, black spruce, Labrador tea, and others. The cut samples were further separated into green leaves and woody material and then dried in a dryer at 70°C for 48 hours. Aboveground dry weights were then measured for the green leaves and woody parts of each species. LMA was quantified to convert aboveground biomass into leaf area. We collected green leaves from seven dominant species near the sixteen quadrats (sample weight 8.2 g ~ 22.2 g in dry mass). The leaves were laid on a transparent sheet without overlap and scanned images were taken. The leaves' images were then converted into black-and-white images to separate the leaves from other pixels. By counting the leafy pixels, we obtained the leaf area of each species. Then, the leaves were dried at 70°C for 48 hours, and their dry weights were recorded. From the ratio of dry weight to leaf area, we obtained the LMA of understory species.

4. Data Records

All ecosystem structure data have been archived and published at the National Institute of Polar Research Arctic Data Archive System (see Data Citations). Data are stored in four directories named "Tree_census", "Tree_allometry", "OverstoryLAI", and "Understory_LAI_biomass". All directories include figures containing the data and R code, to read and output data tables in comma-separated values (CSV) format. In the data files, missing data are recorded as NA.

- Tree_census
    - /Figures
    - TreeCensus.R
    - TreeCensus.csv

      The items recorded are tree location, species name, DBH in the year 2010, tree height in the year 2010, canopy maximum projections (north, west, south, east) in the year 2010, lowest green foliation height in the year 2010, DBH in the year 2014, tree height in the year 2014.

- Tree_allometry
    - /Figures
    - /Photos
    - Tree_allometry.R

- allometry_summary.csv

  This file contains the summary of vertically integrated values. The record from 22 trees is summarized.

- Branch_drymass_profile.csv

  Vertical profiles of dry biomass of dead and live branches in each 50-cm interval are recorded.

- Leafarea_profile.csv

  Vertical profiles of green leaf area in each 50-cm interval are recorded.

- Leafmass_profile.csv

  Vertical profiles of green leaf biomass in each 50-cm interval are recorded.

- stem_drymass_profile.csv

  Vertical profiles of stem biomass in each 50-cm interval are recorded.

- stem_diameter_profile.csv

  Vertical profiles of stem diameter in the lowest, middle and top portions of each 50-cm interval are recorded.

- OverstoryLAI
  - /Figures
  - /Photo

    Upward and downward photographs at the gap fraction measurement locations are stored. The file names “A1.jpg”, “A1up.jpg”, and “A1dn.jpg” indicate location view, upward and downward images in the sampling location at the first point of line A. The line names and location numbers correspond to those in the data file “GapFraction_20180724.csv”

  - /Geolocation_shape

    Geolocation data for all gap fraction measurements are recorded as GIS vector data (point data). The file format is an ESRI shape file.

  - GapFraction_20180724.R
  - GapFraction_20180724.csv

    Gap fraction measurements along four transects (A, B, C, and D) are recorded in five view directions (ring 1 to ring 5).

  - PAI_20180724.csv

    Landscape-scale plant area index (PAI) and leaf area index (LAI), as calculated through the methods described in Section 3.3.

  - SkyCondition_20180724.csv

    These are ancillary data used in PAI and LAI estimation through the methods described in 3.3.

- Understory_LAI_biomass
    - /Figures
    - /Photos
    - Understory_LAI_biomass.R
    - location_info.csv

        Geolocation of 16 quadrat sites in latitude/longitude (WGS 84) and Universal Transverse Mercator (UTM) zone 6N (Easting/Northing)
    - Understory_LAI_biomass.csv

        LAI and total biomass are recorded as well as green leaf and woody biomass of cloudberry, cotton grass, bog bilberry, cranberry, bog birch, black spruce, Labrador tea, and others.
    - LMA.csv

        LMA of seven dominant species are recorded.

5. Technical Validation

5.1. Forest census survey

In the 2014 forest census survey, to confirm consistency with the 2010 observations, the data obtained were immediately compared with the 2010 data on site. If the measurements were inconsistent, suggesting potentially erroneous values, we measured the sample again.

5.2. Aboveground biomass of black spruce trees and understory LAI and LMA measurements

All collected data were first recorded in a field notebook and digitized. The data were transcribed to spreadsheets and double-checked by another individual. All data were plotted and visually checked for consistency.

5.3. Forest gap fraction and overstory LAI

Forest gap fraction measurements at each location were taken twice (from east to west and west to east) to confirm that the results were consistent. We visually checked the consistency of the two measurements and then averaged their values at each sampling point.

6. Competing interests

The authors declare that they have no competing interests.

7. Figures

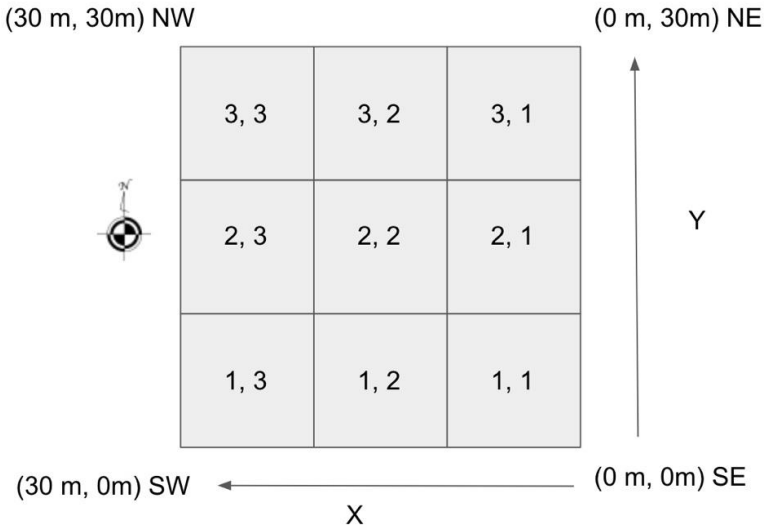

Figure 1. Coordinates of the forest census 30 m × 30 m plot containing nine 10 m^2 subplots. The origin is located at the southeast corner.

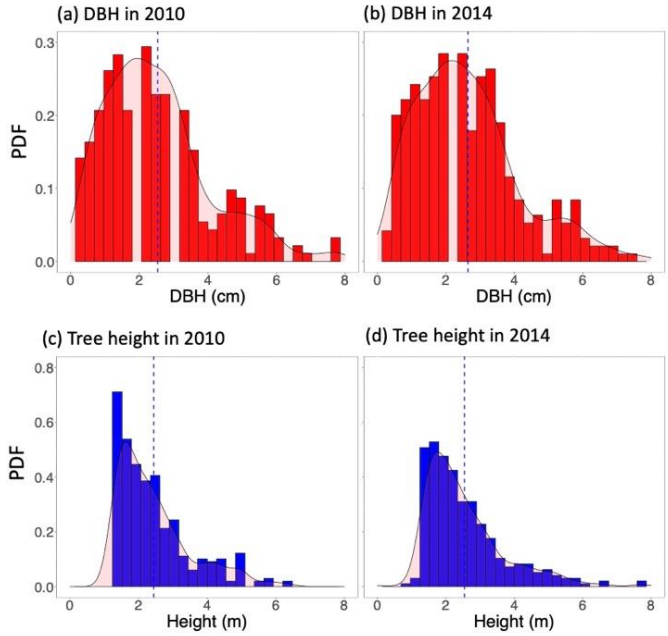

Figure 2. The histograms of DBH and tree height. The pink-shaded curves are fitted with Probability distribution functions (PDF). (a) DBH in 2010, (b) DBH in 2014, (c) height in 2010, and (d) height in 2014. Dashed blue vertical lines indicate average values. The histograms of DBH and tree height are normalized to 1 to compare with the PDF function.

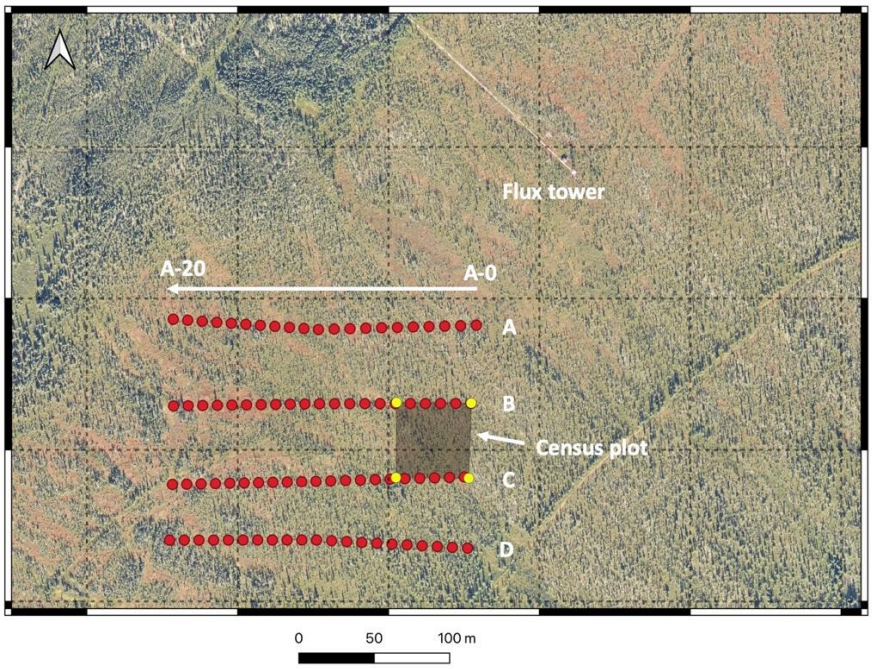

Figure 3. Sampling locations of the gap fraction along four 200 m transects (A, B, C, D). The transects were established in an east–west direction to represent optimally the gap fraction in the southern direction, near the sun's position. The sampling locations are at a 10 m interval. A gray rectangle with yellow dots in the corner is the location of the census measurements. The orthogonal aerial photograph was obtained from the NEON Airborne Observatory Program.

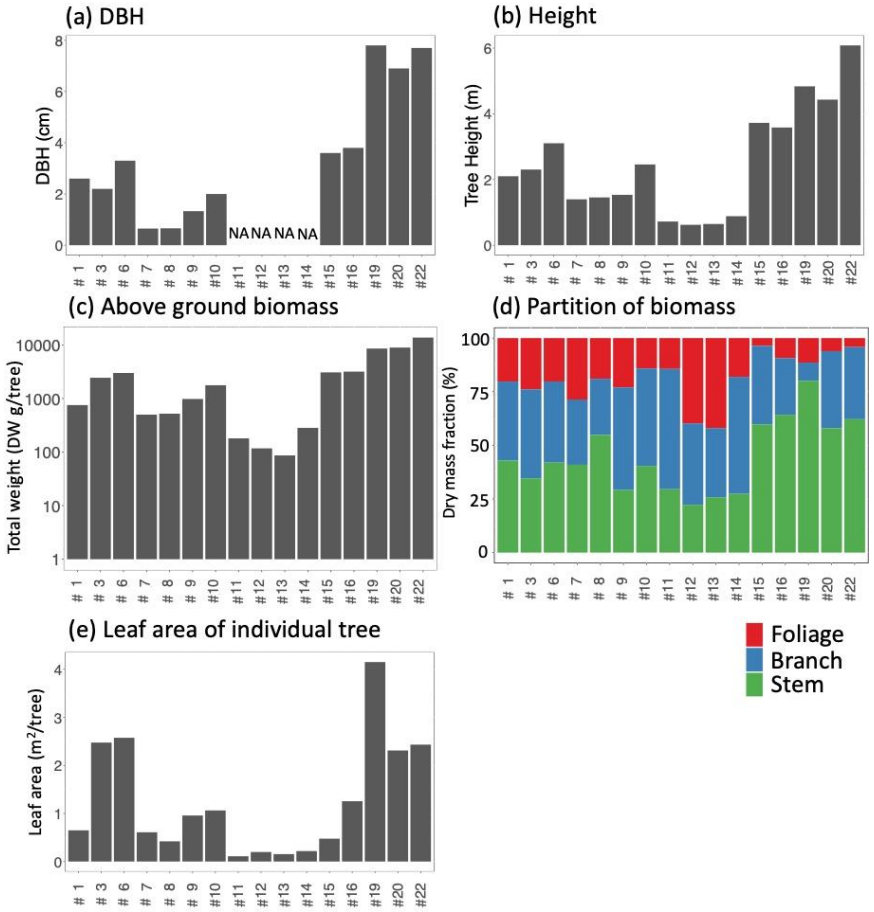

Figure 4. Summary of tree observations. (a) DBH, (b) tree height, (c) aboveground dry biomass, (d) partitions of tree biomass (foliage, branch and stem), and (e) total leaf area of each tree. The X-axis represents the sample tree ID. The tree ID 2, 4, 5, 17, 18, 21 are omitted from the figures because destructive sampling was not performed. Tree IDs 11, 12, 13, and 14 were shorter than the height of DBH measurements; thus, DBHs were not shown.

8. Tables

Table 1. A list of existing micrometeorological and plant phenology monitoring in the study site.

Variable	location	Instrument	Starting year
CO_2 and water fluxes	Scaffold tower at the height of 11 m & tripod at 1.9 m	Infrared gas analyzer (LI-7200, LiCOR) and sonic anemometer (WindMasterPro, Gill)	October, 2010
Meteorological data	Various height 0 to 17 m	Temperature/humidity sensor (HMP155, Vaisala), Longwave/shortwave radiation sensor (CNR-4, Kipp&Zonen) Wind Speed (010C, MetOne) etc	October, 2010
Time lapse camera	Scaffold tower at the height of 17 m & tripod at 1.0 m	PEN camera system (Nikon Coolpix 4300 and fish-eye lens)	January, 2011
Spectral reflectance	Scaffold tower at the height of 17 m & tripod at 1.5 m	MS-700 (Eko)	March, 2015

Table 2. Description of LAI-2200C data. The time zone is Alaska Standard Time (AKST, UTC-0900). The times shown are the start times of transect measurement. With the 45° sensor view cap opening toward the sun, the sensor azimuth would be 0°. The solar azimuth angle is measured clockwise from true north.

Transect ID	Date	Time	Solar zenith angle [°]	Solar azimuth angle [°]
A	Jul 24, 2018	16:40	58.12	246.58
B	Jul 24, 2018	16:29	57.07	243.78
C	Jul 24, 2018	16:08	55.14	238.30
D	Jul 24, 2018	15:43	52.99	231.53

Table 3. Input variables for LAI calculation. The leaf reflectance and transmittance, and fraction of beam radiation are values at the wavelength of 450 nm, which is used in LAI-2200C measurements.

Variable name	Value
Leaf reflectance	0.0535
Leaf transmittance	0.0128
Solar zenith angle	57.07
Solar azimuth Angle	243.78
View azimuth angle	157.5
Fraction of beam radiation	0.736
Shoot clumping	1.58
Element clumping index (apparent clumping index)	0.78
Woody fraction	0.16
LAI	0.88

Author contributions

HK, RS, YK, TN, HI, SN, KN, WY, and AH designed the measurement protocol. HK, RS, YK, TN, HI, SN, KN, WY, AH, and SM contributed to the collection of field measurements. HK, KI, and SN analyzed the data. All members contributed to manuscript preparation.

Acknowledgments

This work was conducted as part of the Arctic Challenge for Sustainability (ArCS) & ArCSII Project (JPMXD1420318865), JAMSTEC-IARC/UAF collaboration studies (JICS), JAXA Earth Observation Research Announcement (RA 6 PI #111, ER2GCF105, and ER3GCF103), JSPS Grant-in-Aid for Scientific Research 19K12294, 20H00640, 20KK0263, 20K12146, 21H05317, and a National Research Foundation of Korea Grant from the Korean Government (MSIT; the Ministry of Science and ICT, NRF-2021M1A5A1065425) (KORI-PN23011, CAPEC Project). We thank Patric Graham, Katie Nagel, and Hannah Pryce for fieldwork assistance with the tree sampling project, Tomoharu Inoue of JAMSTEC for fieldwork assistance with the forest census project, Takeshi Doi

(Hokkaido University), NSF Research Experiences for Undergraduates (REU) Internship IARC coordinator Katie Spellman, and the participants Bobbi Bevacqua, Pacifica (Kitrea) Takata-Glushkoff and Thomas Marrone for fieldwork assistance. All works were conducted in the Poker Flat Research Range of the Geophysical Institute, University of Alaska, Fairbanks. We appreciate the PFRR crew, Kathe Rich, Robert Valdez, Dave Hill, and all other crew members who maintained the flux site infrastructure, the flux site technical manager Bob Busey of IARC/UAF, IARC/UAF director Hajo Eicken and Vice Chancellor of Research at UAF Larry Hinzman for their continuous support and flux site coordination. This paper is dedicated to the late Dr. Rikie Suzuki, our esteemed colleague.

References

1. AMAP. Snow, Water, Ice and Permafrost. Summary for Policy-makers. Arctic Monitoring and Assessment Programme (AMAP), Oslo, Norway, 2017, 20 p.
2. IPCC, 2021: Climate Change 2021: The Physical Science Basis. Contribution of Working Group I to the Sixth Assessment Report of the Intergovernmental Panel on Climate Change [Masson-Delmotte, V. et. al. (Eds.)]. Cambridge University Press. 2023, 2391 p. https://doi.org/10.1017/9781009157896.
3. Box, J. E. et al. Key indicators of Arctic climate change: 1971–2017. Environ. Res. Lett. 2019, 14, 045010. https://doi.org/10.1088/1748-9326/aafc1b.
4. Smith, S. L. et al.. The changing thermal state of permafrost. Nat. Rev. Earth Environ. 2022, 3, p. 10–23. https://doi.org/10.1038/s43017-021-00240-1.
5. IARC. Alaska's Changing Wildfire Environment. https://uaf-iarc.org/alaskas-changing-wildfire-environment/ (accessed 2023-05-01).
6. Fisher, J. B. et al. Missing pieces to modeling the Arctic-Boreal puzzle. Environ. Res. Lett. 2018, 13, 020202. https://doi.org/10.1088/1748-9326/aa9d9a.
7. Nakai, T. et al. Characteristics of evapotranspiration from a permafrost black spruce forest in interior Alaska. Polar Sci. 2013, 7 (2), p. 136–148. https://doi.org/10.1016/j.polar.2013.03.003.
8. Ikawa, H. et al. Understory CO_2, sensible heat, and latent heat fluxes in a black spruce forest in interior Alaska. Agric. For. Meteorol. 2015, 214–215, p. 80–90. https://doi.org/10.1016/j.agrformet.2015.08.247.
9. Sugiura, K. et al. Supersite as a common platform for multi-observations in Alaska for a collaborative framework between JAMSTEC and IARC. JAMSTEC Rep. Res. Dev. 2011, 12, p. 61–69. https://doi.org/10.5918/jamstecr.12.61.
10. Kobayashi, H. et al. In Situ Observations Reveal How Spectral Reflectance Responds to Growing Season Phenology of an Open Evergreen Forest in Alaska. Remote Sensing, 2018, 10 (7), 1071. https://doi.org/10.3390/rs10071071.
11. Nagai, S. et al. 8 million phenological and sky images from 29 ecosystems from the Arctic to the tropics: the Phenological Eyes Network. Ecol. Res. 2018, 33, p. 1091–1092. https://doi.org/10.1007/s11284-018-1633-x.

12. Ueyama, M. et al. Does summer warming reduce black spruce productivity in interior Alaska? J. Forest Res. 2015, 20 (1), p. 52–59. https://doi.org/10.1007/s10310-014-0448-z.
13. Noguchi, K., Dannoura, M., Jomura, M., Awazuhara-Noguchi, M., and Matsuura, Y. High belowground biomass allocation in an upland black spruce (*Picea mariana*) stand in interior Alaska. Polar Sci. 2012, 6 (1), p. 133–141. https://doi.org/10.1016/j.polar.2011.12.002.
14. Kobayashi, H. et al. Spectral reflectance and associated photograph of boreal forest understory formation in interior Alaska. Polar Data J. 2018, 2, p. 14–29. https://doi.org/10.20575/00000004.
15. Nagai, S. et al. Seasonal changes in camera-based indices from an open canopy black spruce forest in Alaska, and comparison with indices from a closed canopy evergreen coniferous forest in Japan. Polar Sci. 2013, 7 (2), p. 125–135. https://doi.org/10.1016/j.polar.2012.12.001.
16. Kobayashi, H. et al. Latitudinal gradient of spruce forest understory and tundra phenology in Alaska as observed from satellite and ground-based data. Remote Sens. Environ. 2016, 177, p. 160–170. https://doi.org/10.1016/j.rse.2016.02.020.
17. Ryu, Y. et al. On the correct estimation of effective leaf area index: Does it reveal information on clumping effects? Agric. For. Meteorol. 2010, 150 (3), p. 463–472. https://doi.org/10.1016/j.agrformet.2010.01.009.
18. Ryu, Y. et al. How to quantify tree leaf area index in an open savanna ecosystem: A multi-instrument and multi-model approach. Agric. For. Meteorol. 2010, 150 (1), p. 63–76. https://doi.org/10.1016/j.agrformet.2009.08.007.
19. Kobayashi, H., Ryu, Y., Baldocchi, D. D., Welles, J. M., and Norman, J. M. On the correct estimation of gap fraction: How to remove scattered radiation in gap fraction measurements? Agric. For. Meteorol. 2013, 174–175, p. 170–183. https://doi.org/10.1016/j.agrformet.2013.02.013.
20. Chen, J. M., Rich, P. M., Gower, S. T., Norman, J. M., and Plummer, S. Leaf area index of boreal forests: Theory, techniques, and measurements. J. Geophys. Res. Atmos. 1997, 102 (D24), p. 29429–29443. https://doi.org/10.1029/97JD01107.
21. Kobayashi, H., Suzuki, R., Nagai, S., Nakai, T., and Kim, Y. Spatial Scale and Landscape Heterogeneity Effects on FAPAR in an Open-Canopy Black Spruce Forest in Interior Alaska. IEEE Geosci. Remote. Sens. Lett. 2014, 11 (2), p. 564–568. https://doi.org/10.1109/LGRS.2013.2278426.

Data Citations

Kobayashi, H., Kim, Y., Nakai, T., Ikawa, H., Nagai, S., Noguchi, K., Yang, W., Hama, A., Matsumura, S., Ikeda, K., and Suzuki, R. Ecosystem structure data sets of an open canopy black spruce forest in Interior Alaska for ecosystem modeling. 1.00, Japan, Arctic Data archive System (ADS), 2023. https://doi.org/10.17592/001.2023050101.